JOURNAL OF THERMOPHYSICS AND HEAT TRANSFER
Vol. 9, No. 4, October–December 1995

# Analysis of Forced Convection Heat Transfer in Microencapsulated Phase Change Material Suspensions

Yuwen Zhang* and Amir Faghri†
*University of Connecticut, Storrs, Connecticut 06269-3139*

**A numerical solution of laminar forced convection heat transfer of a microencapsulated phase change material suspension in a circular tube with constant heat flux has been presented in this article. Melting in the microcapsule was solved by a temperature transforming model instead of a quasisteady model. The effects of the microcapsules crust, the initial subcooling, and the width of the phase change temperature range on the variation of the dimensionless tube wall temperatures, along the axial direction, were also considered in the present model. The agreement between the present numerical results and the experimental results is very good.**

## Nomenclature

$B$ = constant in Eq. (23)
$Bi_p$ = Biot number of particle, $h_p r_p/k_p$
$C$ = heat capacity, J/(m³K)
$C^*$ = dimensionless heat capacity, $C_p/C_b$
$c$ = volumetric concentration
$E$ = term in Eq. (1), J/m³
$E^*$ = term in Eq. (10), $E/(C_b q R_d/k_b)$
$e$ = velocity gradient, 1/s
$Fo$ = Fourier number, $\alpha_b t/r_p^2$
$h_p$ = convection heat transfer coefficient on the particle, W/(m²K)
$K_p$ = dimensionless thermal conductivity of microcapsule, $k_p/k_b$
$k$ = thermal conductivity, W/(mK)
$L$ = latent heat of the PCM, J/kg
$m$ = constant in Eq. (23)
$Nu_p$ = Nusselt number on particle, $h_p r_p/k_b$
$Pe$ = Peclet number, $2R_d u_m/\alpha$
$q$ = heat flux, W/m²
$R$ = circular duct radial coordinate, m
$R_d$ = radius of circular duct, m
$Re$ = Reynolds number, $2R_d u_m/\nu_f$
$r$ = microcapsule radial coordinate, m
$r^*$ = dimensionless radial coordinate of particle, $r/r_p$
$r_c$ = radius of PCM core, m
$r_p$ = radius of particle, $m$
$r_s$ = radius of solid–liquid interface in particle, m
$S$ = dimensionless heat source, $sR_d/q$
$Ste$ = Stefan number, $C_b(qR_d/k_b)/(c\rho_p L)$
$s$ = heat source, W/m³
$T$ = temperature, K
$t$ = time, s
$u$ = velocity in axial direction, m/s
$u_m$ = average velocity in axial direction, m/s
$X$ = dimensionless axial coordinate of circular duct, $x/(R_d Pe_b)$
$x$ = axial coordinate of circular duct, m
$\alpha$ = thermal diffusivity, m²/s
$\Gamma$ = dimensionless effective thermal conductivity of suspensions, $k_e/k_b$
$\Delta T_p$ = phase change temperature range, K
$\varepsilon$ = dimensionless phase change temperature range, $\Delta T/(qR_d/k_b)$
$\eta$ = dimensionless radial coordinate of circular duct, $R/R_d$
$\theta$ = dimensionless temperature, $(T - T_m)/(qR_d/k_b)$
$\rho$ = density, kg/m³

*Subscripts*
$b$ = bulk fluid
$e$ = effective
$f$ = suspending fluid
$i$ = initial or inlet
$m$ = melting point
$p$ = particle
pc = phase change material core of particle
pw = crust of particle
$w$ = tube wall

## Introduction

RECENTLY, a new technique of utilizing phase change material (PCM) in energy storage and control systems has been proposed. In this method, the PCM is microencapsulated and suspended in a heat transfer fluid to form a phase change suspension. Charunyakorn et al.[1] developed a numerical solution of microencapsulated phase change suspension flow between parallel plates for different boundary conditions for low-temperature applications. Following this work, they also published the numerical solution of microencapsulated phase change suspension flow in circular tubes with boundary conditions of constant wall temperature and constant heat flux.[2] Their results showed that the heat transfer in suspension flow is dependent on the bulk Stefan number and volumetric concentration.

In order to evaluate the heat transfer characteristics of phase change suspensions, Goel et al.[3] conducted an experimental study using a suspension of *n*-eicosane microcapsules in water. Their experiments were conducted for laminar, hydrodynamically fully developed flow in a circular tube with a constant heat flux boundary condition. The results showed that the use of a PCM suspension can reduce the rise in wall temperature by up to 50% as compared to a single phase fluid with the same nondimensional parameters. These results agreed qualitatively with the theoretical prediction of Charunyakorn et al.,[2] but quantitative agreement was not good. The differences between the theoretical prediction[2] and experimental results[3] were very large.

The PCM in Goel et al.'s experiments was encapsulated in a crust that made up 30% of the total volume of the microcapsule, but in Charunyakorn et al.'s model, the thickness of the microcapsule's crust was ignored. In order to investigate

Received Feb. 1, 1995; revision received May 15, 1995; accepted for publication May 16, 1995. 

*Research Associate, Department of Mechanical Engineering.
†Professor and Head, Department of Mechanical Engineering. Associate Fellow AIAA.

the effect of microcapsule crust on the wall temperature, Goel et al. compared the result for 15% concentration experiments to Charunyakorn et al.'s 10% concentration results,[2] so that the effective PCM concentrations were similar. This method is not accurate since the thermal resistance of the capsules crust was not taken into account. Charunyakorn et al.[2] also assumed that the suspension enters the test section at the melting point of the PCM. In Goel et al.'s experiments, the temperature of the suspension entering the test section was slightly below the melting point, thus requiring some initial sensible heating before the actual phase change process could take place. Goel et al. suggested that the effect of initial subcooling could be accounted for by considering only the length of the test section where the temperature was equal to or greater than the melting point of *n*-eicosane. This correction is not accurate since it assumed that the entire flow reached the melting temperature at the same location.

After the previous two corrections, the differences between the theoretical prediction[2] and experimental results[3] were still more than 45%. Charunyakorn et al.[2] assumed that all melting occurs exactly at the melting point of the PCM. Roy and Sengupta[4] have studied the properties of microencapsulated PCM and their results clearly show that supercooling occurs during the freezing process. According to this phenomena, Goel et al. believed that the reason for the large difference between the theoretical prediction and experimental results could be the cause of the varying melting temperature of the PCM. Due to the existence of the supercooling phenomena in the freezing process, the PCM in the microcapsules may not be in a completely solid state when the suspension enters the test section. Therefore, the amount of heat absorbed by the microcapsules would be decreased. This may be the most important reason for the large differences between the experimental and the predicted results. In order to simulate this phenomena, the melting process can be assumed to take place over a range of temperatures below the melting point of the PCM.

In Charunyakorn et al.'s papers,[1,2] the amount of heat absorbed by the microcapsules was calculated by Tao's solution for the melting of a sphere.[5] In order to simplify the solution of melting in a sphere, quasisteady assumptions were used by Tao. The drawback of the quasisteady method was that the sensible heat of the PCM was not taken into account so that a higher melting rate would be obtained.[6] On the other hand, the quasisteady method can only account for one-dimensional problems; if initial subcooling exists in the sphere or the melting process takes place over a range of temperatures, the quasisteady method will not apply. Therefore, the first part of this article examines the melting in a subcooled sphere where the microcapsules crust is taken into account. The melting process will not exactly occur at the melting point, but instead takes place over a range of temperatures below the melting point of the PCM. In the second part of this article, the laminar forced convection heat transfer in a microencapsulated PCM suspension is studied numerically. The effect of the microcapsule's crust, initial subcooling, and the range of temperatures for melting will be taken into account. The agreement between the predicted results of this study and the experimental results of Goel et al.[3] is a significant improvement over earlier studies.

## Melting in the Particle

Figure 1 details the regions of a melting sphere of PCM, where the PCM was encapsulated in a wall. The radii of the particle and the PCM core are $r_p$ and $r_c$, respectively. The particle absorbs heat by convection at its outer surface. In order to simplify the melting problem, the following assumptions are made:

1) The initial temperature of the particle is uniform at $T_i$, that is below the melting temperature $T_m$.

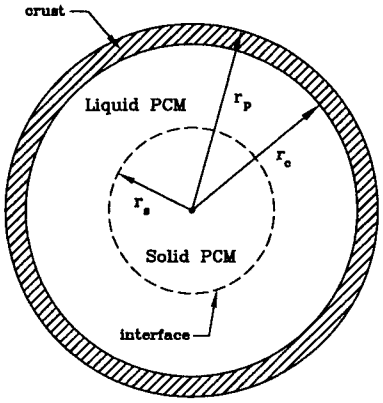


**Fig. 1 Melting in a particle.**

2) The thermal properties of the crust and the PCM core do not vary with temperature.

3) The properties are the same for liquid PCM and solid PCM.

4) The melting takes place over a range of temperatures below $T_m$, where the width of that range is $\Delta T_p$.

The analytical solution of the problem is very complex because of the existence of the particle wall, initial subcooling, and the range of melting temperature. Therefore, a numerical solution using a temperature transforming model with a fixed grid numerical method[7] is used. This model has the advantage of eliminating the time step and grid size limitations that are normally encountered in other fixed grid methods. The governing equation for the wall and PCM core is written as follows:

$$\frac{\partial(C_p T_p)}{\partial t} = \frac{1}{r^2}\frac{\partial}{\partial r}\left(k_p r^2 \frac{\partial T_p}{\partial r}\right) - \frac{\partial E}{\partial t} \tag{1}$$

The thermal properties will take different values for the wall and PCM core.

For the crust ($r_c < r \le r_p$)

$$C_p = C_{\mathrm{pw}} \qquad k_p = k_{\mathrm{pw}} \qquad E \equiv 0 \tag{2}$$

For the PCM core ($0 \le r < r_c$)

$$k_p = k_{\mathrm{pc}} \tag{3}$$

$$C_p(T_p) = \begin{cases} C_{\mathrm{pc}} & \text{if } T_p < T_m - \Delta T_p \\ C_{\mathrm{pc}} + \dfrac{\rho_{\mathrm{pc}} L}{\Delta T_p} & \text{if } T_m - \Delta T_p \le T_p \le T_m \\ C_{\mathrm{pc}} & \text{if } T_p > T_m \end{cases} \tag{4}$$

$$E(T_p) = \begin{cases} C_{\mathrm{pc}}\Delta T_p & \text{if } T_p < T_m - \Delta T_p \\ C_{\mathrm{pc}}\Delta T_p + \rho_{\mathrm{pc}} L & \text{if } T_m - \Delta T_p \le T_p \le T_m \\ C_{\mathrm{pc}}\Delta T_p + \rho_{\mathrm{pc}} L & \text{if } T_p > T_m \end{cases} \tag{5}$$

The boundary conditions and initial condition are

$$-k_{\mathrm{pw}}\frac{\partial T_p}{\partial r} = h_p(T_p - T_f) \quad \text{at} \quad r = r_p, \qquad t > 0 \tag{6}$$

$$\frac{\partial T_p}{\partial r} = 0 \quad \text{at} \quad r = 0, \qquad t > 0 \tag{7}$$

$$T_p = T_i \quad \text{at} \quad t = 0, \qquad r < r_p \tag{8}$$

By defining the following dimensionless variables:

$$\theta_p = \frac{T_p - T_m}{(qR_d/k_b)} \qquad r^* = \frac{r}{r_p} \qquad Fo = \frac{\alpha_b t}{r_p^2}$$

$$\theta_i = \frac{T_i - T_m}{(qR_d/k_b)} \qquad \varepsilon = \frac{\Delta T}{(qR_d/k_b)} \qquad E^* = \frac{E}{C_b(qR_d/k_b)} \tag{9}$$

$$Nu_p = \frac{h_p r_p}{k_b} \qquad C_p^* = \frac{C_p}{C_b} \qquad K_p = \frac{k_p}{k_b}$$

the governing equation, boundary conditions, and initial condition become

$$\frac{\partial(C_p^*\theta_p)}{\partial Fo} = \frac{1}{r^{*2}}\frac{\partial}{\partial r^*}\left(K_p r^{*2}\frac{\partial \theta_p}{\partial r^*}\right) - \frac{\partial E^*}{\partial Fo} \tag{10}$$

$r_c^* < r^* < r_p^*$

$$C_p^* = C_{pw}/C_b \qquad K_p = k_{pw}/k_b \qquad E^* \equiv 0 \tag{11}$$

$0 < r^* < r_c^*$

$$K_p = k_{pc}/k_b \tag{12}$$

$$C_p^*(\theta_p) = \begin{cases} \dfrac{C_{pc}}{C_b} & \text{if } \theta_p < -\varepsilon \\ \dfrac{C_{pc}}{C_b} + \dfrac{1}{cSte\,\varepsilon} & \text{if } -\varepsilon \le \theta_p \le 0 \\ \dfrac{C_{pc}}{C_b} & \text{if } \theta_p > 0 \end{cases} \tag{13}$$

$$E^*(\theta_p) = \begin{cases} \dfrac{C_{pc}}{C_b}\varepsilon & \text{if } \theta_p < -\varepsilon \\ \dfrac{C_{pc}}{C_b}\varepsilon + \dfrac{1}{cSte} & \text{if } -\varepsilon \le \theta_p \le 0 \\ \dfrac{C_{pc}}{C_b}\varepsilon + \dfrac{1}{cSte} & \text{if } \theta_p > 0 \end{cases} \tag{14}$$

$$K_p \frac{\partial \theta_p}{\partial r^*} = Nu_p(\theta_p - \theta) \quad \text{at} \quad r^* = 1, \qquad Fo > 0 \tag{15}$$

$$\frac{\partial \theta_p}{\partial r^*} = 0 \quad \text{at} \quad r^* = 0, \qquad Fo > 0 \tag{16}$$

$$\theta_p = \theta_i \quad \text{at} \quad Fo = 0, \qquad r^* < 1 \tag{17}$$

where, *Ste* in Eqs. (13) and (14) is the Stefan number, which will be defined in Eq. (27).

Equation (10) can be seen as a nonlinear equation of the unsteady heat conduction. The discretization equations are obtained by an implicit finite differential model[8] and solved by the tridiagonal matrix algorithm (TDMA) method. The radius of $r_s$ can be determined after the converged temperature distribution is obtained.

## Heat Transfer in the Suspension

Figure 2 shows a diagram describing the problem. The flowfield in the tube may be divided into two regions: 1) a melting region and 2) a fully melted region. In order to obtain the governing equations of the problem, the following assumptions are made:

1) The microcapsules concentration are less than 0.2 in order that the fluid can be considered as Newtonian.

2) The flow is assumed to be incompressible and laminar. It is also hydrodynamically fully developed and at a uniform temperature below the melting point of the PCM when it enters the heat transfer section.

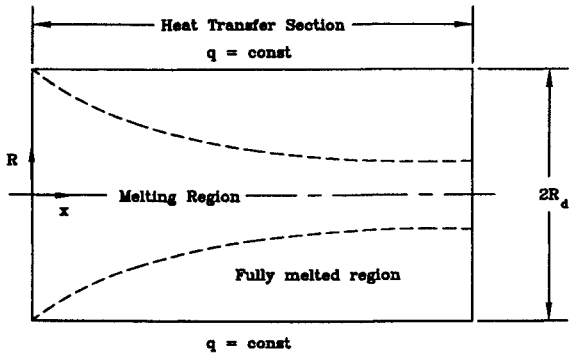


**Fig. 2 Heat transfer in tube.**

3) The particles are considered to be a rigid inert sphere with density approximately equal to that of the suspending fluid.

4) The slurry is assumed to be homogeneous and, therefore, has constant bulk properties, except for the thermal conductivity, which is a function of the local shear and varies across the flowfield.

5) The particle free layer next to the tube wall is assumed to be negligible.

6) The axial conduction of the suspension and the viscous dissipation is neglected.

Based on the previous assumptions, the velocity profile, energy equation, and boundary condition for a constant heat flux at the pipe wall are

$$u = 2u_m[1 - (R/R_d)^2] \tag{18}$$

$$C_b u\frac{\partial T}{\partial x} = \frac{1}{R}\frac{\partial}{\partial R}\left(k_e R\frac{\partial T}{\partial R}\right) + s \tag{19}$$

$$\frac{\partial T}{\partial R} = \frac{q}{k_{ew}} \quad \text{at} \quad R = R_d, \qquad x > 0 \tag{20}$$

$$\frac{\partial T}{\partial R} = 0 \quad \text{at} \quad R = 0, \qquad x > 0 \tag{21}$$

$$T = T_i \quad \text{at} \quad x = 0, \qquad R < R_d \tag{22}$$

where $k_e$ is the effective thermal conductivity of flow slurry, which can be calculated by the following formula[2]:

$$k_e/k_b = 1 + BcPe_p^m \tag{23}$$

where $k_b$ is the bulk thermal conductivity of the slurry. It can be evaluated from Maxwell's relation[1,2]

$$\frac{k_b}{k_f} = \frac{2 + k_p/k_f + 2c(k_p/k_f - 1)}{2 + k_p/k_f - c(k_p/k_f - 1)} \tag{24}$$

The Peclet number of the particle $Pe_p$ found in Eq. (23) is[2]

$$Pe_p = \frac{e(2r_p)^2}{\alpha_f} = 8Pe_f\left(\frac{r_p}{R_d}\right)^2\left(\frac{R}{R_d}\right) \tag{25}$$

The constants $B$ and $m$ in Eq. (23) can be determined from Ref. 2.

The source term $s$ in Eq. (19) can be obtained from the product of the heat absorption rate per particle and the number of particles per unit volume of the slurry. Since the melting

in an encapsulated sphere has been solved in the previous section, the heat absorption rate per particle is expressed as

$$\dot{Q} = -4\pi r_p^2 k_{pw} \left.\frac{\partial T_p}{\partial r}\right|_{r=r_p}$$

The number of particles per unit volume of slurry are

$$N = 3c/4\pi r_p^3$$

Therefore, the source term $s$ in Eq. (19) is

$$s = N\dot{Q} = \frac{3c}{r_p} h_p(T_p|_{r=r_p} - T_f) \tag{26}$$

Finally, by defining the following dimensionless variables:

$$\theta = \frac{(T - T_m)}{(qR_d/k_b)} \qquad X = \frac{x}{R_d Pe_b} \qquad \eta = \frac{R}{R_d}$$

$$U = \frac{u}{u_m} \qquad \Gamma = \frac{k_e}{k_b} \qquad Ste = \frac{C_b(qR_d/k_b)}{c\rho_p L} \tag{27}$$

$$Pe_f = \frac{2R_d u_m}{\alpha_f} \qquad Pe_b = \frac{2R_d u_m}{\alpha_b} \qquad S = \frac{sR_d}{q}$$

Eqs. (19–22) become

$$(1 - \eta^2)\frac{\partial\theta}{\partial X} = \frac{1}{\eta}\frac{\partial}{\partial\eta}\left(\Gamma\eta\frac{\partial\theta}{\partial\eta}\right) + S \tag{28}$$

$$\frac{\partial\theta}{\partial\eta} = \frac{1}{\Gamma_w} \quad \text{at} \quad \eta = 1, \qquad X > 0 \tag{29}$$

$$\frac{\partial\theta}{\partial\eta} = 0 \quad \text{at} \quad \eta = 0, \qquad X > 0 \tag{30}$$

$$\theta = \theta_i \quad \text{at} \quad X = 0, \qquad \eta < 1 \tag{31}$$

where

$$\Gamma = 1 + Bc8^m[Pe_f(r_p/R_d)^2]^m\eta^m \tag{32}$$

$$S = 3c\left(\frac{R_d}{r_p}\right)^2 Nu_p(\theta_p|_{r^*=1} - \theta) \tag{33}$$

In Eq. (33), $\theta_p|_{r^*=1}$ is the dimensionless surface temperature of the particle that depends on the heat transfer process in the microcapsule. It can be determined from the time that the particle enters the tube. This time will depend on the axial and radial coordinates in the circular tube. Since the velocity profile in the tube is fully developed, the dimensionless time $Fo$ in the previous section can be expressed as

$$Fo = \frac{\alpha_b(x/u)}{r_p^2} = \left(\frac{R_d}{r_p}\right)^2 \frac{X}{1 - \eta^2} \tag{34}$$

The convective heat transfer coefficient around the particle can be evaluated from the conduction model based on the thermal conductivity that includes the effects of molecular diffusion and eddy convection around the particles. Therefore, the Nusselt number in Eqs. (15) and (33) can be expressed as follows[2]:

$$Nu_p = \frac{k_p}{k_b} Bi_p = \frac{k_e}{k_b}\frac{2(1 - c)}{(2 - 3c^{1/3} + c)} \tag{35}$$

The heat transfer conservation equation in microencapsulated PCM suspensions have been obtained. The discretization form of Eqs. (28–31) can be obtained by an implicit finite differential method[8] and solved by a TDMA method. However, since the source term in Eq. (28) is an implicit function of the suspension temperature and the axial and radial coordinate, it is necessary to solve this problem by iteration. The dimensionless grid size for $X$ and $\eta$ in the solution procedure are $5 \times 10^{-5}$ and $6.25 \times 10^{-3}$, respectively.[2]

## Results and Discussion

Before studying the heat transfer in a microcapsule PCM suspension, melting in a sphere under the boundary condition of the third kind was solved by a temperature-transforming model.[7] The comparison between the present results and those obtained by a quasisteady model[5] is given in Fig. 3. Since the quasisteady model cannot account for a two-region problem, the initial temperature of the sphere was assumed to be at the melting point of the PCM. The sphere is assumed to be made of pure PCM and the thickness of the capsule crust was assumed to be zero. The environment temperature $T_f$ was assumed to be maintained at a constant value. In order to simulate a sharp melting front, a small temperature range $\Delta T/(T_f - T_m) = 10^{-4}$ is used in the calculations and the initial temperature is set to $(T_i - T_m)/(T_f - T_m) = -10^{-4}$ instead of $(T_i - T_m)/(T_f - T_m) = 0$. The environment temperature $T_f$ satisfies the formulation of $C_c(T_f - T_m)/(\rho_c L) = 0.1$. As can be seen from Fig. 3, the radius of the solid–liquid interface obtained by the quasisteady method is smaller than that obtained by the present model. This means that the melting rate obtained by the quasisteady method is faster than the present numerical solution. In fact, the amount of heat absorbed by the sphere can be divided into two parts: one part is used to supply the latent heat of the melting and the other part is used to increase the temperature of melted liquid. In the quasisteady model, the second part was assumed to be zero. In other words, the heat amount absorbed by the sphere was assumed to be entirely used to supply the latent heat of melting. Therefore, the quasisteady models will result in a higher melting rate. In other words, use of quasisteady models to study heat transfer in microencapsulated PCM suspensions may not yield accurate results.

Figure 4 shows the variation of the tube wall temperature along the axial direction for the suspension entering the tube without initial subcooling. For comparison, the results are presented with the same dimensionless wall temperatures and dimensionless axial distance along the tube as in Ref. 3. The properties of the microcapsules and fluid can be found in Ref. 3. The curves for the results of Charunyakorn et al.[2] and the experimental results of Goel et al.[3] are also presented in Fig. 4 for comparison. For the suspension of microcapsules without crust, it can be seen that the dimensionless temperature obtained by the present model is higher than Charunyakorn et al.'s result[2] over most sections of the tube. This is because

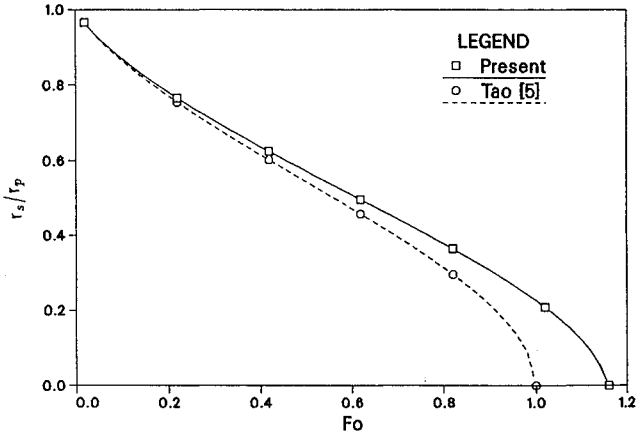


**Fig. 3 Melting front in a PCM sphere.**

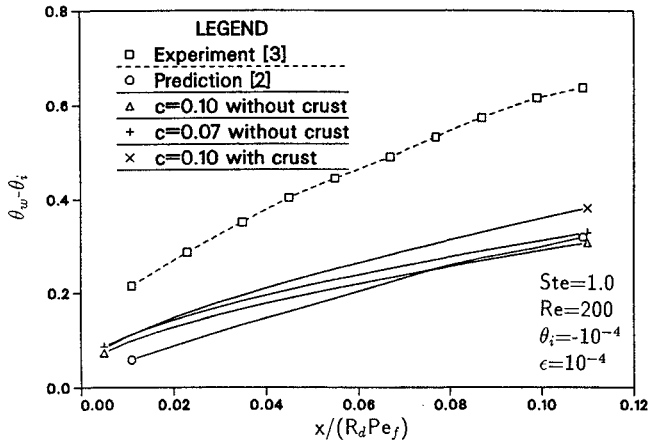


Fig. 4 Effect of the microcapsule crust on dimensionless wall temperature.

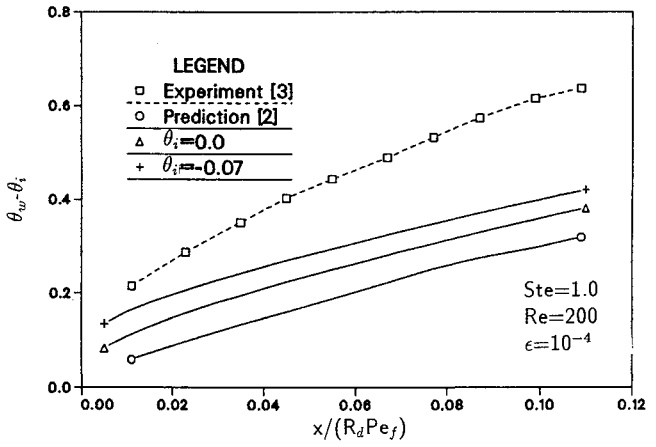


Fig. 5 Effect of initial subcooling on dimensionless wall temperature.

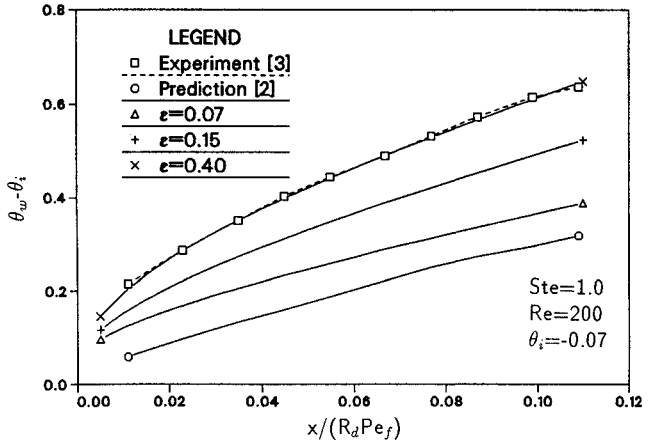


Fig. 6 Effect of the phase change temperature range on dimensionless wall temperature.

the quasisteady method was used to solve the melting of the microcapsules in Charunyakorn et al.'s work[2] and the effect of microencapsulated PCM was exaggerated. For the suspension of microcapsules with a crust that made up 30% of the microcapsules volume, the PCM volume was reduced to 70%. As can be seen, the tube wall temperature was significantly increased when the microcapsule had a crust. In other words, the effect of microcapsules is reduced by the thermal resistance of the crust. The authors of Refs. 1–3 suggest that the effect of the microcapsules crust can be simply treated by defining the concentration based on the actual volume of the PCM. Therefore, the results for a concentration of $c = 0.07$, but without a crust, is also given in Fig. 4. In this case, the actual volume of the PCM is equal to the concentration of $c = 0.1$ with a crust. It can be seen that the difference between the two models is very significant. This is because the thermal resistance of the microcapsule's crust was neglected in Refs. 1–3. Therefore, the suggestion in Refs. 1–3 is not an accurate way of simulating the effect of the microcapsule's crust. The difference between the numerical result and the experimental result can be significantly decreased by the present method.

In Goel et al.'s experiment, the temperature of the suspension entering the test section was below the melting point of PCM, but the initial subcooling of the suspension at the entrance of the test section was not considered in Charunyakorn et al.'s model. The initial subcooling for $Ste = 1.0$ and $c = 0.1$ can be determined by comparing Fig. 4 of this article and Fig. 6 of Ref. 3. It is estimated that the dimensionless temperature of the suspension entering the test section was approximately equal to $-0.07$. Figure 5 shows the effect of the entrance temperature $\theta_i$ on the tube wall temperature. The agreement between experimental result and numerical result can be considerably improved by accounting for the effect of initial subcooling. The differences between the experimental results and the present numerical results are less than 34% instead of the 45% that was found in Ref. 3.

Although the differences between the experimental results and the numerical results were significantly decreased by the present numerical model, it is still very high. Goel et al.[3] thought that the reason for such a large difference was that the melting actually takes place over a range of temperatures instead of only at the exact melting point. Although the supercooling phenomena can be clearly seen during the freezing process of microcapsules, the width of the phase change temperature range was not reported by Roy and Sengupta.[4] Therefore, several phase change temperature ranges are used to calculate the heat transfer in the microencapsulated PCM suspensions. The effects of the varying widths of the phase change temperature range on the tube wall temperature are shown in Fig. 6. The effect of varying the width of the phase change temperature range is very strong. For $\varepsilon = 0.4$, the agreement between experimental result[3] and present numerical result is very good. It is confirmed that the most significant reason for the large difference between Goel et al.'s experimental results[3] and Charunyakorn et al.'s numerical results[2] is that melting takes place over a range of temperatures below the melting point. For $Ste = 1.0$, $c = 0.1$, the dimensionless width of the phase change temperature range, $\varepsilon = 0.4$, is equivalent to the dimensional width of phase change temperature range, $\Delta T = 2.3°C$, which means that the melting takes place over a range of temperatures from 34.4 to 36.7°C. However, this range of phase change temperatures should be examined and established for different PCMs by further experimental work, in order to find an accordingly appropriate value of $\varepsilon$ that can be used in the mathematical models.

## Conclusions

A mathematical model has been developed for the problem of the heat transfer of a microencapsulated PCM suspension flow in a circular duct with constant heat flux. Some of the previous models[2] shortcomings have been identified and corrected by the proposed model of this article. The temperature-transforming model was employed to solve the melting in the microcapsule. The results show that if a quasisteady method is used to simulate the melting in the microcapsules, the effect of microcapsules on the heat transfer of the suspension will be exaggerated. The effect of the microcapsule crust on the heat transfer is also accounted for in the present model. Due to the effect of the thermal resistance of the microcapsule crust, this effect cannot be simply accounted for by defining the concentration based on the actual volume of PCM without the crust. After considering the effect of the microcapsule's

crust and initial subcooling, the difference between the present numerical results and the experimental results are reduced from 45% in Ref. 3 to 34%. The effect of the width of the phase change temperature range was also studied. The results show that the effect of microencapsulated PCM on the forced convective heat transfer in a tube can be significantly reduced by increasing the width of phase change temperature range. However, it is necessary to better determine the width of the phase change temperature range by further experimental work.

## References

[1]Charunyakorn, P., Sengupta, S., and Roy, S. K., "Forced Convection Heat Transfer in Microencapsulated Phase Change Material Slurries: Flow Between Parallel Plates," *General Papers: Phase Change and Convective Heat Transfer*, American Society of Mechanical Engineers HTD-Vol. 129, 1991, New York, pp. 52–62.

[2]Charunyakorn, P., Sengupta, S., and Roy, S. K., "Forced Convection Heat Transfer in Microencapsulated Phase Change Material Slurries: Flow in Circular Ducts," *International Journal of Heat and Mass Transfer*, Vol. 34, No. 3, 1991, pp. 819–835.

[3]Goel, M., Roy, S. K., and Sengupta, S., "Laminar Forced Convection Heat Transfer in Microencapsulated Phase Change Material Suspensions," *International Journal of Heat and Mass Transfer*, Vol. 37, No. 4, 1994, pp. 593–604.

[4]Roy, S. K., and Sengupta, S., "An Evaluation of Phase Change Microcapsules for Use in Enhanced Heat Transfer Fluids," *International Communication of Heat and Mass Transfer*, Vol. 18, No. 4, 1991, pp. 495–507.

[5]Tao, L. C., "Generalized Numerical Solutions of Freezing a Saturated Liquid in Cylinders and Spheres," *AIChE Journal*, Vol. 13, No. 1, 1967, pp. 165–169.

[6]Alexiades, A., and Solomon, A. D., *Mathematical Modeling of Melting and Freezing Process*, Hemisphere, Washington, DC, 1993, pp. 125–153.

[7]Cao, Y., and Faghri, A., "A Numerical Analysis of Phase Change Problems Including Natural Convection," *Journal of Heat Transfer*, Vol. 112, No. 3, 1990, pp. 812–816.

[8]Patankar, S. V., "Elliptic System: Finite-Difference Method I," *Handbook of Numerical Heat Transfer*, Wiley, New York, 1988, pp. 215–290.